

**EXPERIMENTAL INVESTIGATION OF TURBULENCE AND DISPERSION  
AROUND AN ISOLATED CUBIC BUILDING**

*Annalisa Di Bernardino<sup>1</sup>, Paolo Monti<sup>1</sup>, Giovanni Leuzzi<sup>1</sup>, Fabio Sammartino<sup>1</sup> and Simone Ferrari<sup>2</sup>*

<sup>1</sup>Dipartimento di Ingegneria Civile Edile e Ambientale, Università di Roma “La Sapienza”, Roma, Italy

<sup>2</sup>Dipartimento di Ingegneria del Territorio, Università di Cagliari, Cagliari, Italy.

**Abstract:** This paper presents results from experiments conducted in the water channel to investigate turbulence and dispersion around an isolated, cubic obstacle in a neutrally-stratified boundary layer. Pollutant emission is simulated by means of three point sources, located in the vicinity of the cube. Velocity and concentration measurements are carried out at evenly spaced vertical planes, so as to reconstruct the three-dimensional pollutant plume. Here, preliminary results referred to the vertical section passing through the middle plane of the cube are presented. From the instantaneous values of the pollutant concentration, high-spatial resolution maps of mean, variance, intensity and skewness factor of the concentration field have been determined.

**Key words:** *Water channel; Image analysis; Isolated cubic building; Tracer concentration; Point source; 3D plume.*

## **INTRODUCTION**

Investigation of wind flow and turbulent dispersion of passive tracers in urban areas is generally a difficult task because of the complexity of the geometries found in situations of practical interest (see e.g. Pelliccioni et al., 2003). For this reason, studies around single and regular groups of obstacles have been frequently considered by researchers in order to understand the basic characteristics of the flow in rural and urban environments (Cantelli et al., 2015). The isolated cubic obstacle, i.e. one of the simplest geometrical configurations generally considered as an archetype for the study of pollutant dispersion around industrial plants, has frequently been used for testing computational fluid dynamics (CFD) codes. Besides, in many cases such as the isolated cube or street canyon flows, the concentration fluctuations must be also taken into account since the standard deviation of concentration is comparable to the mean concentration values (e.g. Yee et al., 1994).

Recent improvements in CFD have led to the investigation of pollutant dispersion with high spatial resolution (Tominaga, 2017, Jadidi et al., 2016, Mavrodis et al., 2015, Tominaga, 2015, Gousseau et al., 2013). However, the results generally depend on the turbulence model, mesh design and boundary conditions, amongst other things. On the other hand, the experimental approach has proved to be a useful tool for determining flow and dispersion around obstacles using both wind and water channels (Pournazeri et al., 2013, Pardyjak et al., 2001, Iizuka, 2008). However, experimental data are usually provided only for a few points of interest or, at most, for vertical or horizontal planes passing through the source. For these reasons, the reconstruction of the three-dimensional fields of the statistical moments of pollutant concentration and velocity measured with high spatial resolution can be useful, for example, for the validation of CFD codes or Lagrangian dispersion models (e.g. Pelliccioni et al., 1997; Amicarelli et al., 2011; Amicarelli et al. 2012).

In this work, an isolated, cubic building is immersed in a neutrally-stratified boundary layer, reproduced in a water-channel facility. The dispersion of a passive tracer is studied for three different positions of a point source. The experiments show the capability of the apparatus in determining spatial inhomogeneities of the mean, variance, intensity and skewness of the pollutant concentration fields.

## **EXPERIMENTAL SETUP**

The experiments are performed in a close-loop water channel located at the Hydraulics Laboratory of the University of Rome – La Sapienza. The channel is 7.4 m long, 0.25 m wide and 0.35 m high. A fully-developed neutral boundary layer is recreated increasing the surface roughness by means of small pebbles that cover the channel bottom upstream of the test section. For all the experiments, the water depth is  $h=0.16$  m and the free-stream velocity is  $U=0.33$  m s<sup>-1</sup>. The Reynolds number of the flow,  $Re=U \cdot h/\nu$ , is nearly 50,000 ( $\nu=10^{-6}$  m<sup>2</sup> s<sup>-1</sup> is the kinematic viscosity of water). More details on the experimental apparatus can be found in Di Bernardino et al. (2015a) and (2015b). The isolated cubic obstacle ( $B=W=H=20$  mm) is placed on the middle section of the channel ( $y=0$ ), 5 m downstream of the inlet, where the boundary layer can be considered as fully developed. Pollutant emission is simulated by releasing by gravity a solution of Rhodamine-WT and water from a circular source with 1 mm inner diameter. The concentration at the source is  $c_0=2.5 \times 10^{-3}$  kg m<sup>-3</sup>, while the mass flow rate is  $10^{-3}$  kg s<sup>-1</sup>. Three different point source locations (Figure 1), aligned along the middle section of the channel, are considered: (i) ground-level ( $z=0$ ) source and  $x=-0.75H$ , (ii)  $z=H$  and  $x=0$ , (iii)  $z=0$  and  $x=0.75H$ .

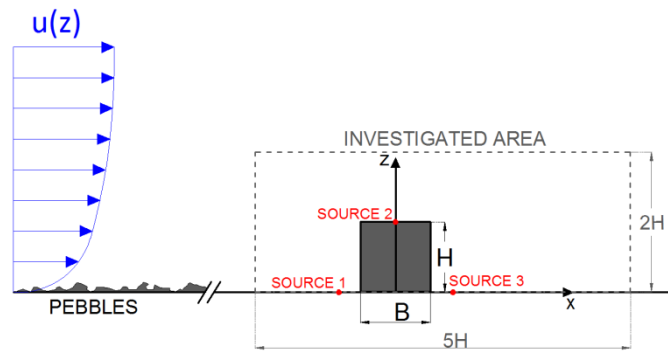


**Figure 1.** Side view of the test area. The locations of the three sources are also shown.

Following the assessment of the repeatability of the flow conditions by performing the same experiment several times, a first experiment was conducted in order to measure the velocity field. The investigated area was 0.10 m long ( $x$ -axis) and 0.04 m high ( $z$ -axis) and was illuminated by a 5 W green laser sheet (wavelength 532 nm). Images captured by a 8-bit CMOS-camera (1280x1024 pixels in resolutions) acquiring 250 frames per second for 80 seconds permitted the instantaneous velocity field to be evaluated along the  $x$ - $z$  plane by a feature-tracking algorithm based on image analysis. Velocities were deduced from particle displacements between successive frames and interpolated on a regular grid by Gaussian averaging. In this way, the experiment allowed us to analyze 20,000 instantaneous velocity fields with 1 mm spatial resolution.

Three additional experiments were conducted to measure the instantaneous concentration fields via planar laser-induced fluorescence (PLIF) for the three source positions using a 10-bit CMOS-camera (2352x1728 pixels in resolutions). The resolution of the concentration field is the pixel size, i.e.  $8 \cdot 10^{-5}$  m.

In order to reconstruct the three-dimensional velocity and concentration fields, velocity and concentration measurements are carried out for 50 different vertical planes, parallel to the streamwise direction, and separated by 1 mm along the  $y$ -axis.

## RESULTS

In what follows, results concerning the statistical moments of the pollutant concentration referred to the vertical plane passing through the middle section of the obstacle are presented. To better understand the dispersion mechanism, it may be helpful to give a brief description of the velocity field along the  $x$ - $z$  plane. Figure 2 shows a vector representation of the mean velocity field. The flow pattern conforms to the classical configuration expected for a three-dimensional isolated cube (e.g. Fackrell's, 1984; Martinuzzi and Tropea, 1993), i.e. a horseshoe vortex near the ground wrapping around the cube and bending along the streamwise direction. The flow separates at the upwind edges, producing separation zones on the roof top and on the lateral sides of the building. At the downwind edges the flow separates again, producing the cavity region with a bow vortex. Only a partial signature of this complex flow is discernible in Figure

2. The length of the upstream vortex is slightly less than  $H$ , measured from the windward façade of the obstacle, while the reattachment point of the bow vortex downwind of the cube is at  $\approx 1.4H$  from its leeward façade. The mean velocity field is in qualitative agreement with numerical outcomes from Mavroidis et al. (2015) and Santos et al. (2009), among others.

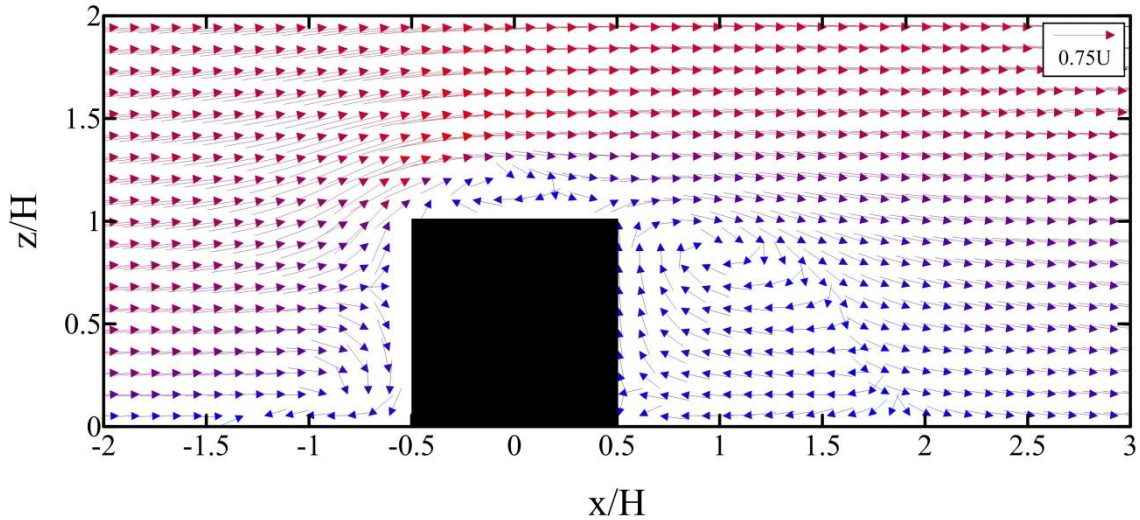


**Figure 2.** Vector plot of the mean velocity at  $y=0$ .

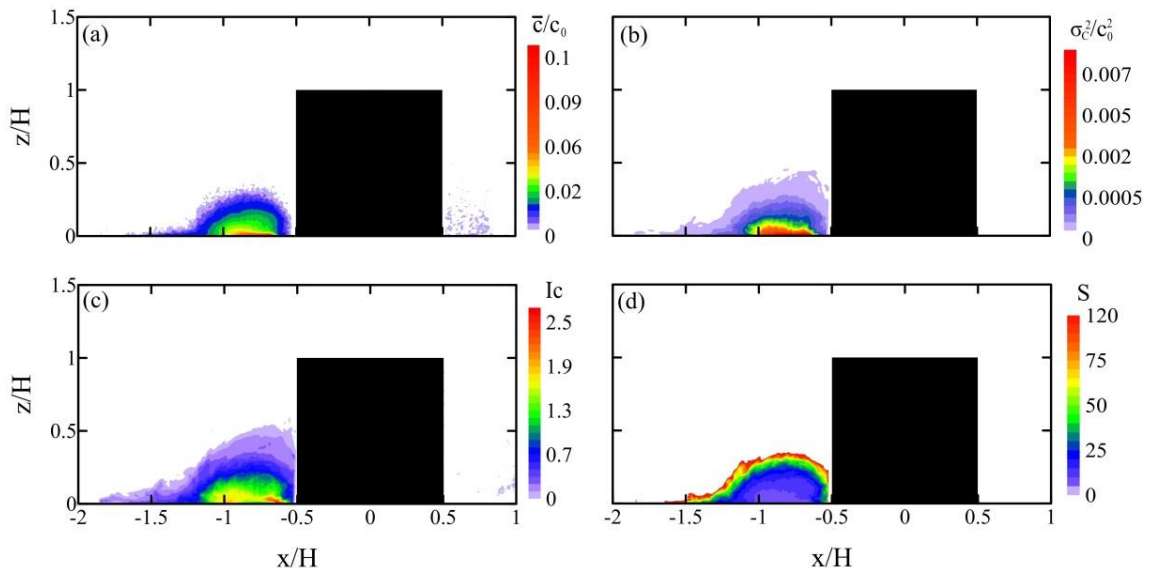


**Figure 3.** Mean (a), variance (b), intensity (c) and skewness (d) of the non-dimensional pollutant concentration for the source located at  $x=-0.75H$ ,  $z=0$  and  $y=0$ .

Figures 3, 4 and 5 show the (non-dimensional) concentration statistics obtained for the three point source locations. When the source is upwind of the building (Figure 3), the pollutant is partially advected upstream and remains mainly trapped within the horseshoe vortex (see the non-dimensional concentration field depicted in Figure 3a). Then, the tracer moves laterally and is carried downwind. Similarly, when the tracer is emitted from the rooftop source (Figure 4), it remains on average confined in the vortex located in the upwind half of the cube top (Figure 4a). The large streamwise velocity of the flow limits the extension of the plume to  $z/H=1.3$ . In Figure 5 the downwind, the case of the ground-level source is investigated. The map of  $\bar{c}/c_0$  is quite different from those seen for the two previous source locations: the mean concentration (Figure 5a) shows much lower values because of the higher pollutant dilution caused by the bow vortex.

The trends of the non-dimensional variance,  $\sigma_c^2/c_0^2$ , intensity of concentration,  $I_c = \bar{c}/\sigma_c$ , and Skewness factor,  $S = \overline{c'^3}/\sigma_c^3$ , are similar for the three cases: the variance and the intensity of concentration follow the propagation of the plume and assume higher values near the source, i.e. where the concentration decreases rapidly and higher gradients occur. The Skewness factor gives a measure of the asymmetry of the concentration distribution. As expected for a quantity limited below, it assumes only positive values. Near the source, where the pollutant recirculates continuously,  $S$  assumes lower values, while it increases at the plume boundaries, i.e. where the pollutant is seldom present. For all the three source locations, the asymmetry of the concentration distribution is not negligible and, therefore, it might play a significant role in the dispersion process.

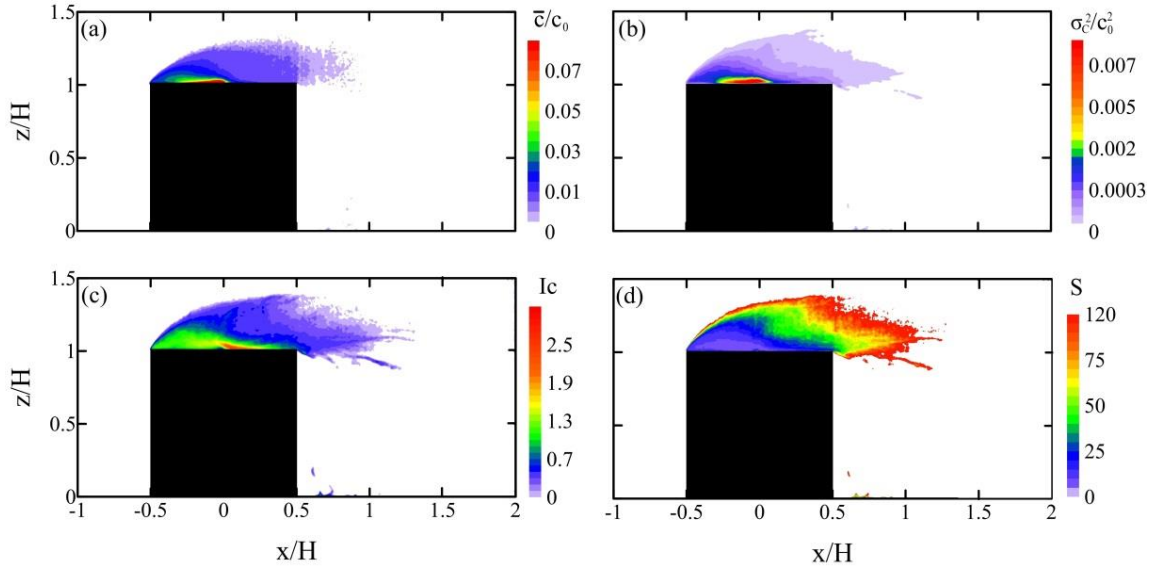


Figure 4. As in Figure 3, but for the source located at the center of the building roof.

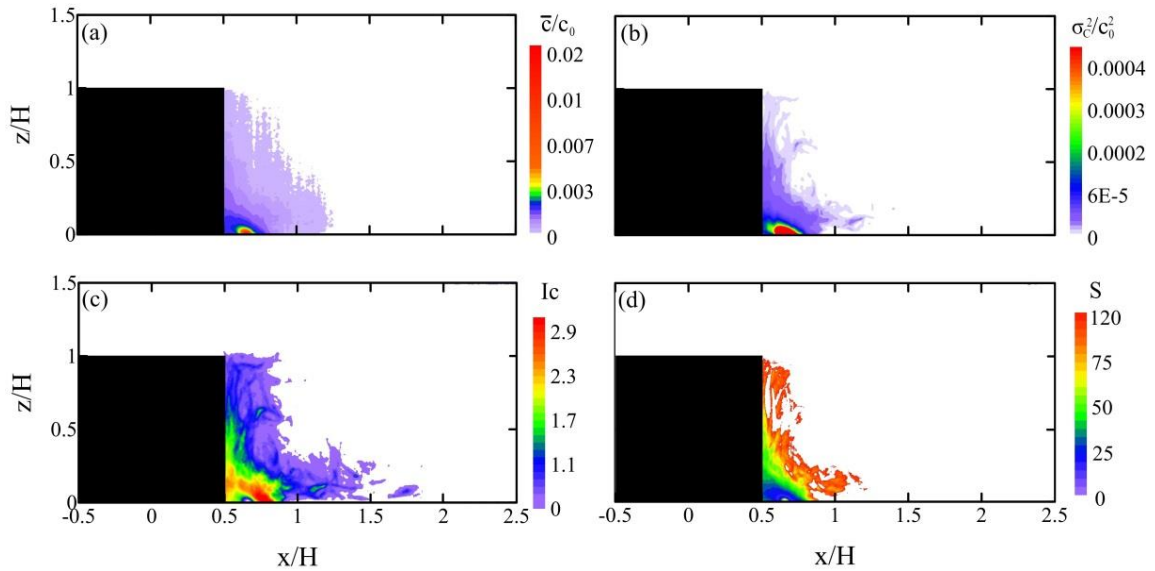


Figure 5. As in Figure 3, but for the source located at 0.25H downwind of the building.

## CONCLUSIONS

Concentration measurements have been carried out to investigate experimentally the dispersion of a passive tracer emitted from a point source in the vicinity of an isolated, cubic building. Three different source locations have been considered in order to analyse situations typically observed in real cases.

The facility seems to be suitable for studying turbulence and dispersion with high spatial resolution. The image analysis technique has allowed the reconstruction of the average concentration field as well as of the variance, intensity and Skewness factor of the concentration. This work has to be seen as a starting point for subsequent analysis concerning the whole three-dimensional velocity and concentration fields around an isolated building.

## REFERENCES

- Amicarella, A., G. Leuzzi, P. Monti, D.J. Thomson, 2011: A comparison between IECM and IEM models, *Int. J. Environ. Pollut.*, **47**, 324-331.
- Amicarella, A., P. Salizzoni, G. Leuzzi, P. Monti, L. Soulhac, F.-X. Cierco, F. Leboeuf, 2012: Sensitivity analysis of a concentration fluctuation model to dissipation rate estimates, *Int. J. Environ. Poll.*, **48**, n.1/2/3/4, 164-173.
- Cantelli, A., P. Monti, G. Leuzzi, 2015: Numerical study of the urban geometrical representation impact in a surface energy budget model. *Environ. Fluid Mech.*, **15**, 251-273.
- Di Bernardino, A., P. Monti, G. Leuzzi and G. Querzoli, 2015a: A laboratory investigation of flow and turbulence over a two-dimensional urban canopy. *Boundary-Layer Meteorol.*, **155**, 73-85.
- Di Bernardino, A., P. Monti, G. Leuzzi and G. Querzoli, 2015b: On the effect of the aspect ratio on flow and turbulence over a two-dimensional street canyon. *Int. J. Environ. Pollut.*, **58**, 27-38.
- Di Bernardino, A., P. Monti, G. Leuzzi and G. Querzoli, 2017: Water-channel estimation of Eulerian and Lagrangian time scales of the turbulence in idealized two-dimensional urban canopies. *Boundary-Layer Meteorol.*, **165**, 251-276.
- Fackrell, J., 1984: An examination of simple-models for building influenced dispersion, *Atmos. Environ.*, **18**, 89-98.
- Gousseau, P., B. Blocken, G.J.F. van Heijst, 2013: Quality assessment of Large-Eddy Simulation of wind flow around a high-rise building: validation and solution verification, *Comput. Fluids*, **79**, 120-133.
- Iizuka, S., H. Kondo, K. Muto, A. Hori, K. Kitabayashi, T. Mizuno, 2008: A wind-tunnel study on gaseous diffusion around a building within two different atmospheric boundary layers. In: *Proceedings of the 4th International Conference on Advances in Wind and Structures (AWAS'08)*. Jeju, Korea, May 20-31, 2008.
- Jadidi, M., F. Bazdidi-Tehrani, M. Kiamansouri, 2016: Embedded large eddy simulation approach for pollutant dispersion around a model building in atmospheric boundary layer, *Environ. Fluid Mech.*, **16**, 575-601.
- Martinuzzi, R., C. Tropea, 1993: The flow around surface-mounted, prismatic obstacles placed in a fully developed channel flow: (data bank contribution), *J. Fluids Eng.*, **115**, 85-92.
- Mavroidis, I., S. Andronopoulos, A. Venetsanos, J. G. Bartzis, 2015: Numerical investigation of concentrations and concentration fluctuations around isolated obstacles of different shapes. Comparison with wind tunnel results, *Environ. Fluid Mech.*, **15**, 999-1034.
- Pelliccioni, A., 1997: The Gram-Charlier method to evaluate the probability density function on monodimensional case. *Nuovo Cimento C*, **20**, 435-452.
- Pelliccioni, A., C. Gariazzo, T. Tirabassi, 2003: Coupling of neural network and dispersion models: A novel methodology for air pollution models. *Int. J. Environ. Pollut.*, **20**, 136-146.
- Pournazeri, S., N. Schulte, S. Tan, M. Princevac, A. Venkatram, 2013: Dispersion of buoyant emissions from low level sources in urban areas: water channel modelling, *Int. J. Environ. Pollut.*, **52**, 119-140.
- Santos, J.M., N.C. Reis Jr., E.V. Goulart, I. Mavroidis, 2009: Numerical simulation of flow and dispersion around an isolated cubical building: The effect of the atmospheric stratification, *Atmos. Environ.*, **43**, 5484-5492.
- Tominaga, Y., 2015: Flow around a high-rise building using steady and unsteady RANS CFD: Effect of large-scale fluctuations on the velocity statistics, *J. Wind Eng. Ind. Aerod.*, **142**, 93-103.
- Tominaga, Y., T. Stathopoulos, 2017: Steady and unsteady RANS simulations of pollutant dispersion around isolated cubical buildings: Effect of large-scale fluctuations on the concentration field, *J. Wind Eng. Ind. Aerod.*, **165**, 23-33.
- Yee, E., R. Chan, P.R. Kosteniuk, G.M. Chandler, C.A. Biltoft, J.F. Bowers, 1994: Incorporation of internal fluctuations in a meandering plume model of concentration fluctuations, *Boundary-Layer Meteorol.*, **67**, 11-38.